Proton transfer in surface-stabilized chiral motifs of croconic acid

Donna A. Kunkel, James Hooper, Scott Simpson, Geoffrey A. Rojas, Stephen Ducharme, Timothy Usher, Eva Zurek, and Axel Enders

Proton transfer in surface–stabilized chiral motifs of croconic acid

Donna A. Kunkel,[1] James Hooper,[2] Scott Simpson,[2] Geoffrey A. Rojas,[1,3]
Stephen Ducharme,[1,4] Timothy Usher,[5] Eva Zurek,[2,*] and Axel Enders[1,4,†]

[1]*Department of Physics and Astronomy, University of Nebraska - Lincoln, Lincoln, NE 68588*
[2]*Department of Chemistry, State University of New York at Buffalo,*
331 Natural Sciences Complex, Buffalo, NY 14360
[3]*Center for Nanophase Materials Science, Oak Ridge National Laboratory,*
One Bethel Valley Road, Oak Ridge, Tennessee 37831
[4]*Nebraska Center for Materials and Nanoscience, University of Nebraska, Lincoln 68588-0298*
[5]*Department of Physics, California State University, San Bernardino,*
5500 University Parkway, San Bernardino CA 92407
(Dated: October 19, 2012)

The structure and cooperative proton ordering of two-dimensional sheets of croconic acid was studied with scanning tunneling microscopy and first-principles calculations. Unlike in the crystalline form, which exhibits a pleated, densely packed polar sheet structure, the confinement of the molecules to the surface results in hydrogen-bonded chiral clusters and networks. First principles calculations suggest that the surface stabilizes networks of configurational isomers, which arise from direct hydrogen transfer between their constituent croconic acid monomers. Some of these configurations have a net polarization. It is demonstrated through constrained molecular dynamics simulations that simultaneous proton transfer between any two molecules can occur spontaneously. This finding is a prerequisite for the occurrence of in-plane ferroelectricity based on proton transfer in 2D sheets.

The recent discovery of ferroelectricity in crystalline croconic acid (CA), $C_5H_2O_5$, has drawn attention to topological organic ferroelectrics [1–3]. In bulk crystal form, CA is a hydrogen bonded, order-disorder ferroelectric with a large room temperature polarization (21 μC/cm^{-2}) and low coercive field (11 kV/cm^{-1}). An applied electric field results in cooperative proton tautomerism, where the electric dipole is reversed via hydroxyl proton displacement along the ferroelectric c-axis [4]. This distinguishes topological, or proton-ordered, organic ferroelectrics from other organic ferroelectrics such as vinylidene fluoride (VDF) [5], which require reorientations of large molecules in an applied electric field to switch the electric polarization and usually exhibit a high coercive field beyond 1200 kV/cm^{-1}. Potassium dihydrogen phosphate, KH_2PO_4, or KDP, is one of the prototype hydrogen bonded inorganic ferroelectrics [6, 7]. Here, the proton ordering in the $a-b$ plane is accompanied by a displacement of the potassium and phosphorous ions along the ferroelectric c axis, making a 3-dimensional crystal structure a prerequisite for ferroelectricity to occur. The electric dipoles are associated with the ions, and not the protons directly [8]. By contrast, crystals of CA form stacked, pleated hydrogen-bonded sheets of molecules with in-plane dipoles, where the polarizations of all sheets are aligned. Each molecule transfers two hydroxyl protons to the carbonyl groups of adjacent molecules within the same sheet, changing the topology of the π-electron system and with it the polarization of each molecule [1, 9]. This implies that for ferroelectricity to occur in proton transfer systems such as CA, 3-dimensional crystal structures are not required [2, 4]. There is potential importance of surface-supported 2D ferroelectrics for applications, including memories, logic devices, printable electronics and organic spintronics. Such development calls for the fundamental, molecular-level understanding of the material properties so that they can be engineered as needed. Here we studied two-dimensional, hydrogen-bonded layers of CA on Ag(111) substrates. We investigated their self-assembly and cooperative proton tautomerism with scanning tunneling microscopy (STM) and first principles calculations. Remarkably, we find that CA self-assembles into chiral nanostructures and networks, which can potentially be useful for the study of polarization ordering in 2D and 3D structures, the role of different packing schemes, and the influence of a substrate on structure and polarization. Our first-principles calculations demonstrate that the substrate can modify the energy barrier for proton transfer and promote polarization ordering in some of the structures investigated.

Two-dimensional structures of CA were synthesized by molecular beam epitaxy on crystalline Ag(111) surfaces under ultrahigh vacuum. The sample was held at room temperature during deposition of the molecules, and cooled to 77 K for imaging with an Omicron Nanotechnology low-temperature STM. At low sub-monolayer coverage, the surface was covered in scattered triangular-shaped clusters, as shown in Fig. 1(a). Croconic acid monomers were identified from unfrequent, pseudo-stable isolated trimers to be the individual lobes in (a). From this follows that CA dimers are the elementary building block for all structures observed, and that each of the
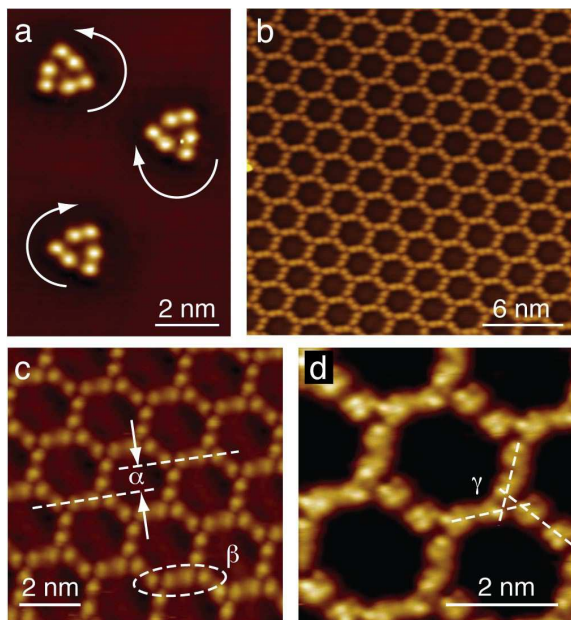
FIG. 1: Scanning tunneling microscopy images of croconic acid on Ag(111). (a) Triangular hexamers where the arrows indicate the chirality. (b-d) 2D extended networks. See text for explanation of features α, β, and γ

triangular-shaped clusters is formed of 3 such dimers. Upon increasing the coverage to close to one full monolayer, followed by weak annealing to 350 K, honeycomb-type 2D networks as in Fig. 1(b) were formed. Images of varied zoom level such as those in Figs. 1(b, c) reveal important structural details of the networks, labelled with α, β, and γ, which will be discussed later. Our observations with STM suggest that the molecules diffuse across the surface, nucleating into dimers which compose the triangular hexamer clusters. At increased coverage the hexamers coalesce, followed by slight rearrangement of the elementary dimers to form the extended 2D networks.

In order to obtain a molecular-level model of the observed structures, density functional theory (DFT) calculations which account for dispersion were carried out (see the supplemental information, SI, for details). The molecular computations were performed using the DFT-D3 [10] functional. The monomer i in Fig. 2(a) was found to be 190 meV/molecule lower in energy than ii in the gas phase, in agreement with the results presented in Ref. [11]. Since experiments [12] have shown that the bulk crystal is comprised of the higher–energy monomer ii, it was also considered. The dimerization energy was computed as being 290 and 340 meV/molecule for dimers i_2 and ii_2, respectively, with the former being lower in energy by 140 meV/molecule. These dimers, and others (see the SI), are the potential building blocks of the hexamers in the low coverage STM images, so they were employed in order to identify structural candidates consistent with the ones shown in Fig. 1(a).

The lowest-energy hexamer found in our computations was configuration i_6 in Fig. 2(b). Rotating the intramolecular C–OH bonds affords a somewhat less stable hexamer ii_6, which, like hexamer i_6, can readily be used to build a model honeycomb lattice that agrees with the high coverage STM image, see Fig. 2(d). Hexamers i_6' and ii_6', on the other hand, best resemble the triangular motifs observed at lower coverage in the STM images. Like their i_6 and ii_6 counterpart hexamers which describe the higher coverage regimes, i_6' and ii_6' are composed of three dimeric building blocks, but are 54-66 meV/molecule higher in energy. Since clusters of type i_6' or ii_6' are the only observed species at lower coverage in the STM images, it is likely that the actual energy difference between the configurations is different on a surface.

Significant charge reorganization can occur upon molecular adsorption, so that the dipole moment of the molecule/adsorbate system cannot be assumed to be the same as the molecular dipole. We have previously illustrated this through our molecular calculations of a quinonoid zwitterion adsorbed to Cu(111) [13], as well as 4-fluorostyrene on both Cu(111) and Au(111) [14]. With regards to the present system our molecular calculations show that a system consisting of a single CA molecule adsorbed on a two layer cluster composed of 166 Ag atoms maintains an appreciable in–plane dipole component of $\sim$1.1 D (see the SI).

It is interesting to note that the 2D arrangements of CA molecules do not resemble the pleated–sheet structure and local molecular arrangement in the bulk crystals. An important consequence of the proposed structures is that they are chiral with respect to the surface. The chirality of a CA molecule of type ii results from the orientation of the two hydroxyl groups, while molecules of type i are not chiral. The dimer ii_2 can only be formed from two molecules of the same chirality. The triangular clusters observed at low coverage consist of 3 dimers containing molecules only of the same type, and are chiral themselves, also when the atomistic structure of the molecules is ignored, as indicated by the arrows in Fig. 1(a). Interestingly, this chirality can be achieved with the chiral molecule ii as well as with the non-chiral molecule i, as the hexamer models i_6' and ii_6' in Fig. 2(c) show.

Extended, two-dimensional networks were constructed from both hexamers, i_6 and ii_6 and are shown in Fig. 2(d). There are distinctive structural differences between these, which we can use to identify the nature of the 2D networks in Fig. 1. The symmetry of both networks is described by the wallpaper group $p6$. They both lack reflection symmetry if the atomistic structure is considered, which implies that they are chiral in 2D. Characteristic for network ii_n is that molecular dimers on opposite corners of the hexagonal unit cell are not aligned with respect to one another (α), 4 molecules on each side of the hexagons appear to be aligned along a linear chain (β) and lines connecting the dimers at the nodes of the
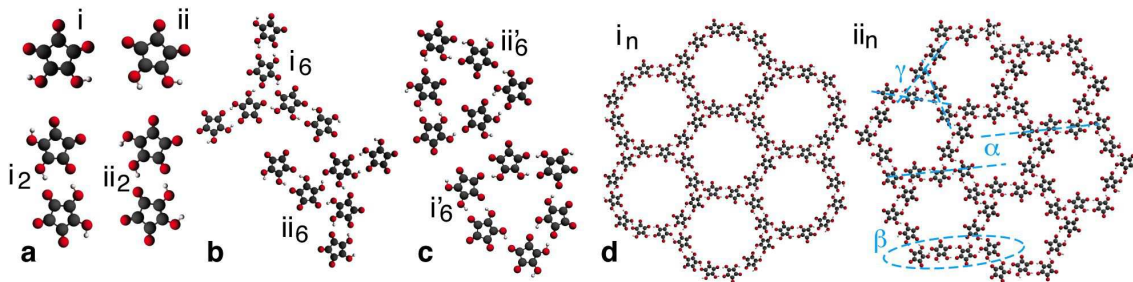
FIG. 2: Structures of plenary croconic acid monomers, dimers and hexamers, as obtained using first-principles calculations (a-c). The 2D networks in (d) were constructed from the hexamers in (b). The features α, β, and γ are highlighted for comparison with the experiment, see Fig. 1.
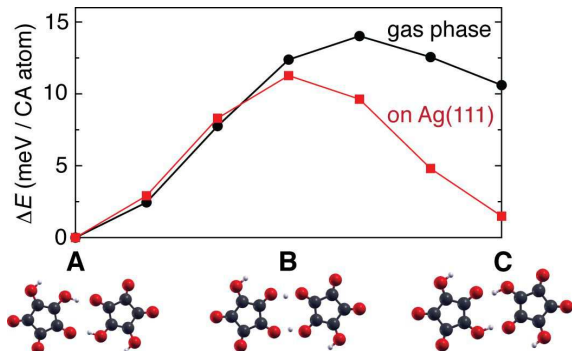

FIG. 3: Relative energies of hydrogen transfer pathway from dimer (ii_2), or **A**, to **C** calculated using DFT-D2 and a periodic program. The points along the pathway were taken from a linear interpolation of the position between **A** and **C**.

network do not meet at the center of the nodes (γ). Careful comparison of those features with the STM images in Fig. 1(b, c) shows that the experimentally observed structures must be of type ii_n. The molecules forming it must therefore be of type ii. Network ii_n can be constructed to be left-handed or right-handed. The network in Fig. 1 contains only left-handed CA molecules ii. It should be noted that we also observed networks of type i_n (see SI), albeit with much lower frequency.

From the close binding distance between the molecules and the uniform chirality, control over the hydrogen transfer and dipole moments becomes possible in the 2D sheets. In order to study this further, we have carried out periodic computations on 2D structures using planewave basis sets, the PAW method, and the DFT-D2 [15] functional. This includes the intermolecular transfer of hydrogen atoms, which is the key mechanism for the occurrence of ferroelectricity in crystalline CA. Here we focus only on structures containing the chiral molecules of type ii, as those were experimentally observed on surfaces. The calculated energy barrier for the transfer of H-atoms within the building block employed for the high–coverage systems, dimer (ii_2), along the illustrated pathway **A-B-C** is shown both in the gas phase and on Ag(111) in

Fig. 3. While cluster **C** is not particularly stable in the gas phase, it is stabilized by almost 100 meV/molecule on the Ag(111) surface and becomes nearly isoenergetic with dimer **A**. This suggests that motifs which are energetically unfavorable in the gas phase may be stabilized on the surface. The barrier height of approximately 170 meV/molecule, which is comparable with the energy barrier to proton transfer reported for the bulk crystal [1], was reduced only slightly. Similar results were computed for the transfer of H–atoms within the dimer on different–sized surface slabs, and within linear trimer arrangements of CA molecules.

An extended network resembling the configurations observed experimentally at high coverage was constructed, see HC_A in Fig. 4. To look for plausible structural alternatives to HC_A and gain insight into the dynamic behavior of the hydrogen atoms in the honeycomb network, ab–initio molecular dynamics (MD) simulations were carried out. Unconstrained calculations showed that HC_A oscillated substantially out of plane, but remained intact, over the time–scale of the simulation, 5 ps. The first step we took in order to simulate how such a network would behave on a surface was to constrain the atoms to lie in the plane of the honeycomb lattice. A concerted multiple–hydrogen transfer was observed during the MD run. The time dependence of select interatomic distances, which corresponded to intermolecular hydrogen bonds at the outset of the calculation, are shown in Fig. 4(a). The spikes just after 60 fs of simulation time correspond to a concerted hydrogen transfer along the O···H contacts. An optimization of the structure extracted from $t = 70$ fs resulted in HC_C. The velocities increased drastically after the transition, and the final geometry extracted from the simulation (near 130 fs) resulted in HC_B.

HC_B is 50 meV/molecule lower in energy than HC_C in the gas phase, and 170 meV/molecule higher than HC_A. It stands out in particular because the dipole moments of its underlying monomers, sketched in Fig. 4(c), do not cancel each other out like they do in HC_A, resulting in a net permanent dipole. Thus, the concerted hydrogen transfer observed was from a configuration with no net
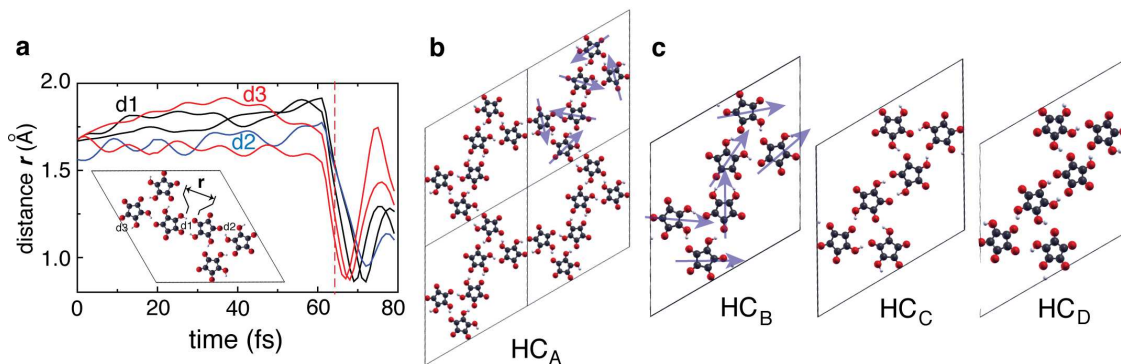
FIG. 4: (a) Select O···H distances in HC$_A$, as labelled in the inset, computed during an ab–initio MD simulation where all of the atoms were constrained to remain in the plane of the honeycomb. The inter and intramolecular OH bond in a CA dimer measures 1.65 and 1.01 Å. (b) A honeycomb network which corresponds to the high–coverage STM images. (c) Three other honeycomb structures which differ mostly in the arrangement of the hydrogen atoms. The direction of the molecular dipoles is indicated with blue arrows. The configuration HC$_B$ exhibits a net dipole.

polarization to a polarized state. The calculated barrier for the collective hydrogen transfer along the pathway HC$_A$ → HC$_B$, similar to Fig. 2, suggests that the substrate stabilizes HC$_B$ to within 45 meV/molecule relative to HC$_A$ (see SI). Ab–initio calculations using the Berry phase method ([16, 17] and references therein) confirm the net dipole moment of HC$_B$ relative to HC$_A$, measuring ∼8 Debye per molecule. This agrees well with the observation that the calculated net dipole of bulk CA is slightly larger than that of its underlying monomers [1]; we calculate the largest dipole for a single monomer in HC$_B$ to be 7.5 Debye. A key difference between CA crystals and the 2D structures in Fig. 4(c), is that stable phases both with and without net polarization may be found only on the surface.

An MD simulation was carried out on HC$_A$ adsorbed on a two layer Ag(111) slab in which the positions of the Ag atoms were constrained, but the CA molecules were allowed to move freely. Although the simulation time we were able to achieve was short (roughly 700 fs), this equilibration nonetheless revealed a hydrogen transfer process after 100 fs to the HC$_D$ structure shown in Fig. 4(c). This structure is roughly 40 meV/molecule lower in energy relative to HC$_A$ using a two layer surface model. Its distinguishing feature is that the number of hydrogen atoms in a single molecule ranges from 1 to 4, instead of always being 2. On the other hand, HC$_D$ was found to spontaneously optimize to HC$_A$ in the gas–phase. Considering the tendency of the DFT-D2 functional to overbind [15], calculations were also performed on the HC$_A$, HC$_B$, HC$_C$, and HC$_D$ structures using the vdW-DF2 functional [18]. The relative energy ranking between the extended neworks better matched that of the gas-phase calculations as expected: for HC$_A$/HC$_B$/HC$_C$/HC$_D$ they were found to be 0/65/38/64 meV/molecule. HC$_A$ remained the most stable honeycomb network, but, unlike in the gas–phase,

the HC$_D$ structure did not spontaneously optimize back to HC$_A$. We believe this illustrates an intriguing possibility in materials design: to engineer the interface such that the system mimics the results of our DFT-D2 calculations and destabilizes the HC$_A$ network relative to, say, HC$_B$.

In conclusion, we demonstrated that two-dimensional sheets of croconic acid molecules, stabilized on Ag(111), exhibit a chiral honeycomb structure that is not observed in the crystalline form. This study thus constitutes an example of how constrained self-assembly, provided here by the layering of the molecules on the surface, makes it possible to control the ordering of hydrogen bonds, in chiral or polar order, for example, within a molecular layer. We have shown through first principles calculations that the the two-dimensional character of the experimentally found structures is not only expected to promote polarization ordering of various kinds, but also that concerted proton transfer to switch the polarization is possible. While experiments demonstrating the proton transfer and the concomitant switching of polarization of the studied structures within the film plane are extremely challenging [4], this study potentially will trigger respective experimental efforts.

* Electronic address: `ezurek@buffalo.edu`

† Electronic address: `aenders2@unl.edu`

[1] S. Horiuchi, Y. Tokunaga, G. Giovannetti, S. Picozzi, H. Itoh, R. Shimano, R. Kumai, and Y. Tokura, Nature **463**, 789 (2010).

[2] S. Horiuchi, R. Kumai, and Y. Tokura, Advanced Materials **23**, 2098 (2011).

[3] A. Stroppa, D. Di Sante, S. Horiuchi, Y. Tokura, D. Vanderbilt, and S. Picozzi, Physical Review B **84**, 014101 (2011).

[4] T. Kumagai, A. Shiotari, H. Okuyama, S. Hatta, T. Aruga, I. Hamada, T. Frederiksen, and H. Ueba, Nature Materials **11**, 167 (2011).

[5] K. Noda, K. Ishida, A. Kubono, T. Horiuchi, H. Yamada, and K. Matsushige, J. Appl. Phys. **93**, 2866 (2003).

[6] J. Slater, J. Chem. Phys. **9**, 16 (1941).

[7] R. Blinck, J. Chem. Phys. **13**, 204 (1960).

[8] R. Levitskii, I. Zachek, A. Vdovych, and S. Sorokov, Condensed Matter Physics **12**, 75 (2009).

[9] S. Horiuchi and Y. Tokura, Nature Materials **7**, 357 (2008).

[10] S. Grimme, J. Antony, S. Ehrlich, and H. Krieg, The Journal of Chemical Physics **132**, 154104 (2010).

[11] C. N. Ramachandran and E. Ruckenstein, Comp. Theor. Chem. **973**, 28 (2011).

[12] D. Braga, L. Maini, and F. Grepioni, CrystEngComm **6**, 1 (2001).

[13] D. Kunkel, S. Simpson, J. Nitz, G. Rojas, E. Zurek, L. Routaboul, B. Doudin, P. Braunstein, P. Dowben, and A. Enders, Chem. Commun. **48**, 7143 (2012).

[14] A. Jewell, S. Simpson, A. Enders, E. Zurek, and C. Sykes, J. Phys. Chem. Lett. **3**, 2069 (2012).

[15] S. Grimme, J. Comp. Chem. **27**, 1787 (2006).

[16] R. Resta, Ferroelectrics **136**, 51 (1992).

[17] R. W. Nunes and X. Gonze, Phys. Rev. B **89**, 155107 (2001).

[18] J. c. v. Klimeš, D. R. Bowler, and A. Michaelides, Phys. Rev. B **83**, 195131 (2011).